Leadership in Sustainable Infrastructure
Leadership en Infrastructures Durables

Vancouver, Canada
May 31 – June 3, 2017/ *Mai 31 – Juin 3, 2017*

EFFICACY OF CONCRETE CONSTITUTIVE MODELS FOR BULLET IMPACT TESTS

Dua, Alok[1,3] and Braimah, Abass[2]
[1,2] Carleton University, Canada
[3] alok.dua@carleton.ca

Abstract: Structures such as defenses/ammunition bunkers in the military and elsewhere are generally constructed at remote locations where concrete structures are more convenient to construct. Such protective structures in most cases are constructed from plain or reinforced concrete due to inherent ease of planning, transportation and construction. The design of these structures is based on field tests which ideally is required to be done for each caliber of weapon for which the protective structure is designed against. Such field tests are time consuming and uneconomical. A cost-effective alternative to field testing is the use of high fidelity physics based numerical modeling techniques. However, constitutive modeling of concrete when subjected to high velocity projectiles is very complex due to factors like material erosion and strain-rate effects. These factors lead to a highly non-linear response, hence, high accuracy of the concrete constitutive model is required to accurately simulate field test results. Commercial finite element software offer various concrete constitutive models. This paper reviews the concrete constitutive models available for modeling bullet impact. Experimental observations from bullet impact on plain concrete with a muzzle velocity (MV) of 900 m/s are presented and used to assess the concrete constitutive models in LS-DYNA. The importance of modeling parameters like strain-rate effects and erosion criteria have been reviewed. It was concluded that *MAT_CSCM (Mat_159) constitutive law was able to accurately simulate the field observations. The numerical results also suggest that an additional increase in the material strength to account for strain-rate effects is inappropriate.

1 Introduction

Over the last few decades a large number of construction materials have been developed for conventional and protective structures. For example sandwich panels, fibre-reinforced composite materials, steel-fibre composites and polymer based materials etc. Concrete however remains the most widely used material in the construction industry. Concrete has distinct advantages over other materials especially at remote locations. The design procedures have matured over time and execution is not complicated. Moreover, the transportation of material required for concrete structures to remote sites is more convenient vis-à-vis transportation of large structural members. Protective structures like firing positions, permanent defenses and ammunition storage bunkers are mostly constructed at remote locations where transportation of large structural members is difficult due to lack of motorable roads. Rear view of a typical firing bunker is shown in Figure 1. Concrete construction becomes the ideal choice for these type of structures. Such structures are designed for protection against small arms fire, direct splinters and overhead protection against air blast/contact blasts. While design of overhead protection against blasts is a different design regime, this article concentrates on projectile impact of concrete.

The level of security provided to the occupants by these structures is of utmost importance. There are international ballistic standards available to quantify the performance requirements/test methods against various small arms (EN-1063, 1999). These standards are however only applicable to civilian structures.

Empirical and analytical methods also exist to predict the penetration resistance of a concrete target. These empirical methods are known to provide inconsistent results and parameters like target stiffness and projectile deformation are not considered (Murthy et al., 2010). Limited literature is available on response of concrete members to projectile impact. This may be due to the fact that field trials involving ballistic/projectile testing has to be conducted in remote areas. In addition, measurement techniques and accurate representation of actual impact loads are required. Consequently, field tests can be expensive and time consuming.

Figure 1: Rear view of a typical concrete firing bunker at a remote location ("Indian Army for Better Frontline Infrastructure," 2014)

Consequently, numerical analysis of these problems have been carried out extensively in the past. However, the validation of such results with experimental data was found to be scarce in the literature. For this study, field trials were carried out for validation purpose. The depth of penetration (DOP), impact face crater diameter (CD) and back face scab diameter (SD) were recorded and compared to numerical simulations carried out with three concrete constitutive models available in LS-DYNA. The objective of the study is to identify an appropriate concrete constitutive model and a set of calibrated parameters that can unambiguously predict the response of concrete due to high strain-rate events like projectile impact and contact explosions. The conclusions from this study are planned to be utilized for further investigation into response of RC members to contact explosions (Dua & Braimah, 2016).

2 Literature Review

A 5.56 mm full metal jacket (FMJ) ball ammunition was used for the experimental tests and accordingly the numerical models have three constitutive materials: concrete, projectile that comprises of a cartridge brass jacket and a lead-antimony alloy core.

2.1 Concrete Constitutive Models

Concrete is a heterogeneous material which implies different behavior for different type of loading which can be in static, quasi-static and high strain-rate regimes. Hence, it is not possible to predict the response with a universal constitutive model. LS-DYNA offers variety of concrete constitutive models capable of predicting realistic response due to shock and impact loads. These include *MAT_PSEUDO_TENSOR (Mat_016), *MAT_GEOLOGIC_CAP_MODEL (Mat_025), *MAT_CONCRETE_DAMAGE_REL3 (Mat_72R3), *MAT_HOLMQUIST_JOHNSON_COOK-HJC (Mat_111), *MAT_WINFRITH_CONCRETE (Mat_084), *MAT_CSCM_CONCRETE (Mat_159) and *MAT_RHT (Mat_272). Each of these models have advantages and disadvantages depending on the loading event. For shock and impact events, a concrete constitutive model should be able to capture the post-peak softening, shear dilation/confinement effect and strain-rate enhancements. In order to capture these effects, various parameters are required to be established by means of laboratory testing. These include tests for uniaxial compression and tensile strength, triaxial compression strength and pressure-volume strain response for equation-of-state. Finite element software users have limited knowledge of these tests and find it time consuming to determine the input parameters required for the models (Wu et al., 2012). Lately, certain models like Mat_72R3, Mat_084 and Mat_159 have simplified this aspect. These models allow auto generation of material constants from the unconfined compressive strength and the density of concrete (User Manual L.S.T.C, 2015). These three

models are specifically developed for analysis of reinforced concrete response to high strain-rate problems like blast and impact. Review of these models have been presented by Chen and Han (1988); Crawford et al. (2011); Murray (2007) and Ottosen (1975).

Wu et al. (2012) presented an analysis of single element simulations carried out with the selected concrete models. The unconfined uniaxial compression and tension simulations from the study show that Mat_084 does not predict the concrete softening. This is contrary to the physical behavior of concrete. Additionally, it cannot capture the confinement effects as shear dilation is not predicted. Mat_72R3 and Mat_159 models capture the strain softening behaviour in compression/tension and the axial force in the confining reinforcement is developed due to shear dilation. Numerical results of a benchmark missile impact on reinforced concrete slab are presented by Dorsselaer et al. (2012). Four material laws: Mat_016, Mat_084, Mat_72R3 and Mat_159 were compared in this study. Mat_72R3 and Mat_159 were found to be appropriate for the study as the spall area and residual missile speed were accurately predicted. Mat_016 and Mat_084 showed large variations from the experimental results. In another work, the Drucker-Prager model, Mat_111, Mat_72R3 and Mat_159 were studied for projectile impact on concrete (Bush, 2010). Mat_111 was found to be more accurate in predicting the perforation criteria observed from experimental results. Recently, a study of damage plasticity models pointed out the importance of well-tuned parameters in material models like Mat_111 and Mat_272, which do not automatically generate material parameters (Pavlovic et al., 2016).

2.2 Constitutive Models for Projectile Materials

FMJ ball ammunition comprises of soft lead core jacketed with brass (Børvik et al., 2009). The brass jacket comprises of 70% Copper and 30% Zinc (CuZn30). The lead core is alloyed with 10% antimony for improved strength. This bullet has limited penetration power due to the highly ductile nature of the lead core, however the projectile invests a large target surface due to deformation. Lead material is difficult to model in Lagrangian domain due to large deformations. Additionally, lead transforms into liquid phase during the impact as its melting point is low. The characteristics of the projectile used are presented in Table 1 and Figure 2.

Table 1: Characteristics of 5.56 mm FMJ ball projectile (Prakash et al., 2015)

Mass g	Jacket thickness mm	Velocity m/s
4.16 ± 0.10	0.35	891 (mean) ± 11.52 (SD)

Prakash et al. (2015) presented the response of steel fibre reinforced cementitious composite (SFCC) panels subjected to 5.56 mm and 7.62 mm calibre FMJ projectiles. The brass jacket was modeled using the Johnson-Cook (JC) material law (Mat_015) while von Mises strength criteria was used for the soft lead-core. Thermal effects and material failure were not considered for the projectile materials, as the subject of study was SFCC. Maréchal et al. (2011) used JC model for the projectile materials without considering failure and heat transfer. Another study on perforation resistance of steel plates against FMJ projectiles used Modified-Johnson-Cook (MJC) model for the cartridge brass jacket and the soft lead core (Børvik et al., 2009). JC material model is widely used for numerical modeling of FMJ ball ammunition (Peroni et al., 2012) however, MJC model has been reported to give more reliable results (Dey et al., 2004). The material parameters for cartridge brass and various other materials as applicable for MJC constitutive law is presented by Johnson and Cook (Johnson & Cook, 1983). Material constants for lead-antimony alloy for MJC model are available in a paper by Børvik et al. (2009). Experimental tests on cartridge brass and lead-antimony alloy were carried out in a study to determine the material parameters calibrated for the JC material law (Peroni et al., 2012). It was concluded that while brass failed at a plastic strain of 30%, failure strain of lead-antimony could not be estimated due to high ductility.

Although, the literature review shows that JC/MJC material laws are appropriate for FMJ projectile impacts, no results were found for FMJ soft lead core projectile impact wherein material damage is considered. The papers found in the literature focus on FMJ steel core bullets that are relatively convenient to model owing to minimal deformation.

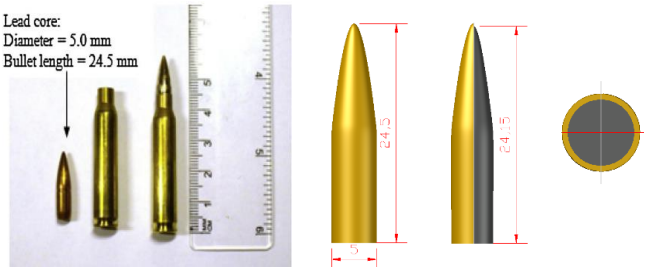

(a) (b) (c) (d)

Figure 2: Physical dimensions of 5.56 mm FMJ ball projectile (a) Projectile and case (Prakash et al., 2015) (b) AUTOCAD model of projectile (c) Cut section (b) Projectile base

3 Experimental Program

3.1 Setup

For the purpose of collecting validation data for the numerical simulations, 12 concrete panels of varying thickness were subjected to projectile impact from a short distance. A standard 5.56 mm calibre weapon was used for the tests. For each thickness of 25 mm, 50 mm, 75 mm and 100 mm, three plain concrete panels of 18 MPa compressive strength were casted to ensure repetition of data.

(a) (b)

Figure 3: Experimental setup (a) Casting of concrete panels (b) Fixing arrangements

The size of panels were 300 x 300 mm and they were placed on a steel frame support. Rotation of the panel edges was allowed in all directions. The weapon was fixed on a bipod at a distance of 2 m as presented in Figure 3-(b). The relative positions of the weapon and the target frame were not altered throughout the tests for all 12 panels to ensure consistency.

3.2 Observations

The 25-mm and 50-mm panels were perforated by the bullet impact while impact face spalling and back face scabbing was observed for the 75-mm panels. No scabbing was observed on the 100-mm panels. Furthermore, one 100-mm panel was subjected to multi-impacts at the same impact location, to check the ballistic limit and it was observed that the panel could take two shots before being perforated by the third one. The crater and scab diameters were recorded for calibration and validation of the numerical results, Table 2 and Figure 4.

Table 2: Results from experimental tests

Panel Thickness (mm)	CD (mm)	Average CD (mm)	DOP (mm)	Average DOP (mm)	SD (mm)	Average SD (mm)
25	48 50 52	50	-	-	62 56 62	60

50	71 67 72	70	-	-	94 87 89	90
75	57 59 64	60	51 57 57	55	118 100 102	110
100	53 59 damaged	56	65 61 damaged	63	-	-

For 75-mm and 100-mm panels, the bullets were trapped within and were completely destroyed as only the fragments could be found. This is in line with previous studies by Børvik et al. (2009) and Dey et al. (2004).

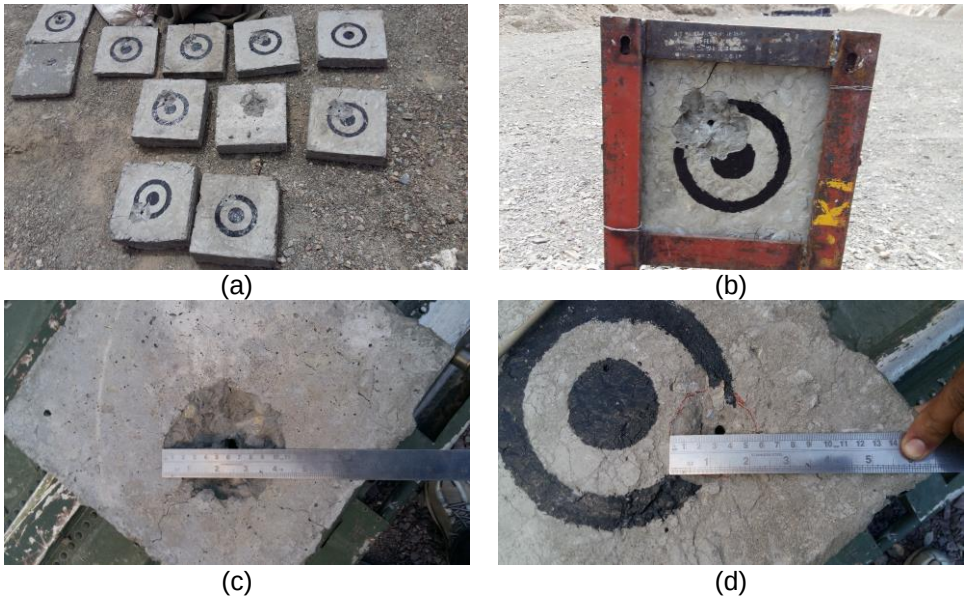

(a) (b) (c) (d)

Figure 4: Spall and scab diameters (a) all panels (b) 75-mm on frame (c) 75-mm (d) 100-mm

4 Numerical Simulations

Quarter symmetric models were created for each thickness of concrete panels. An initial simulation was attempted with MMALE elements for the projectile, however it was realized that solution was not computationally efficient and only Lagrangian elements gave valid results while the element erosion was activated at a constant plastic strain.

4.1 Discretization

The diameter of the 5.56 mm FMJ ball ammunition is 5 mm at the bottom and the brass jacket is 0.35 mm thick. The lead core is free to slide under the brass jacket during the impact and accordingly the nodes of the jacket and core material were not merged (Maréchal et al., 2011). Based on the literature review, the average element size for both the projectile materials was kept 0.25 mm and biased towards the nose, Figure 5. The concrete panel was meshed in two zones based on the experimental observations. A radial zone of 110 mm diameter was meshed with an average element size of 1 mm and biased towards the impact zone (Figure 5-(d)).

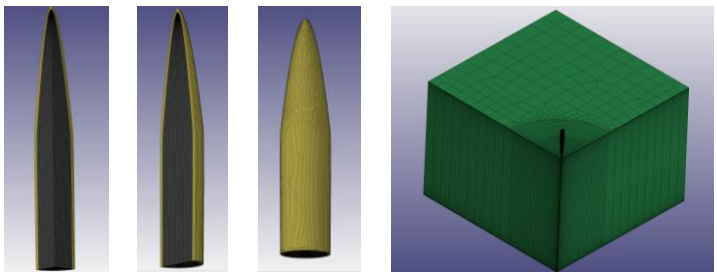

(a) (b) (c) (d)

Figure 5: Discretization of parts (a) Quarter projectile (b) Half projectile (c) Full projectile (d) 100 mm concrete panel

4.2 Strain-Rate Effects

It is an established fact that concrete material exhibit strain-rate dependency. It fails at a higher compressive/tensile load when subjected to a high strain-rate loading compared to its established 28-day strength. In analytical methods, the strength increase is incorporated with a dynamic increase factor (DIF) recommended by various researchers. The same option is available as a parameter for the constitutive models. However, it was observed from preliminary simulations that activating the strain-rate effects is not appropriate. Impact face crater and back face scab are not formed when strain-rate effects are considered. These two phenomenon were observed in the simulation results without considering the strain-rate effects. In another study by the authors, RC slabs were subjected to contact explosion and the numerical results were found to be consistent without rate effects. This aspect has been presented by Schwer (2009). Recently, Williams and Williamson (2011) have highlighted this fact in their study on response of RC columns subjected to blast loading. Thus, strain-rate effect option in the constitutive model has not been activated for the results presented in this paper.

4.3 Material Parameters

The contact between projectile and the concrete panel was implemented with *CONTACT_ERODING_SURFACE_TO_SURFACE, allowing for erosion of damaged elements thereby improving the computational efficiency. The pinball segment based contact that employs penalty forces on the penetrating segments on each surface was used. The segment search option is more efficient than node search for detecting penetration in geometries with sharp edges (LS-DYNA Support, 2016). Sliding between brass jacket and lead core was incorporated with *CONTACT_ERODING_SUFACE_TO_SURFACE between the two parts. The models were initially run with Mat_015 (JC model) and Mat_107 (MJC model). It was soon realized that the projectile eroded completely and results were not obtained. This is due to the thermal softening and excessive deformation of elements in the core. Element erosion and adaptive meshing did not overcome the problem. In view of the objective of this study, *MAT_SIMPLIFIED_JOHNSON_COOK (Mat_098) was chosen wherein the damage and thermal effects are neglected. Erosion of projectile elements was activated at a constant principal strain value of 3. The material properties of cartridge brass and lead-antimony core are presented in Table 3. The model was found to give consistent results for all the thicknesses of concrete panels under consideration. Constant stress Lagrangian solid elements are used for both projectile and the concrete panel.

Table 3: Material constants for Mat_098 model (Børvik et al., 2009)

Material	Density	Elastic Modulus	Poisson's ratio	Rate effects	Yield stress	Strain hardening		Strain-rate hardening		Plastic strain
	ρ (Kg/m^3)	E (MPa)		VP	A (MPa)	B (MPa)	n	ε_0 (s^{-1})	C	FS
Brass	8520	115000	0.35	Deactive	206	505	0.42	5e^{-4}	0.01	3
Lead	10740	16000	0.42	Deactive	24	300	1	5e^{-4}	0.1	3

Three concrete constitutive models have been investigated in this paper: Mat_84, Mat_72R3 and Mat_159. The material constants used for these models are presented in Table 4 while rest of the material parameters were auto-generated. Projectile impact results in large deformations which leads to termination of numerical solution due to negative volume. This problem can be tackled by allowing erosion of highly deformed elements from the solution. An erosion criteria of 15% max principal strain at failure was used in the model (Luccioni et al., 2013; Wilt & Chowdhury, 2011).

Table 4: Material constants for concrete constitutive models

Material	Density	Compressive strength	Poisson's ratio	Tangent modulus	Tensile strength	Rate effects	Erosion criteria	Aggregate size
	Kg/m^3	MPa		MPa	MPa			mm
Mat_72R3	2367	18	-			Off	15%	-
Mat_084	2367	18	-			Off	15%	20
Mat_159	2367	18	0.18	24821	1.4	Off	15%	20

4.4 Numerical Results and Discussion

4.4.1 MAT159: Continuous Surface Cap Model

CSCM model could accurately predict the response observed in experimental tests for all thicknesses. The numerical results presented in Figure 6 show the crater/scab formation which is similar to the field observations.

Table 5: Comparison table for *MAT_CSCM

Observed Parameter	Average Experimental Value (mm)				Numerical Value (mm)				Error (%)			
	25 mm	50 mm	75 mm	100 mm	25 mm	50 mm	75 mm	100 mm	25 mm	50 mm	75 mm	100 mm
CD	50	70	60	56	44	60	60	60	12	14	0	7
DOP	-	-	58	63	-	-	68	68	-	-	17	8
SD	60	90	110	-	50	80	65	-	16	11	40	-

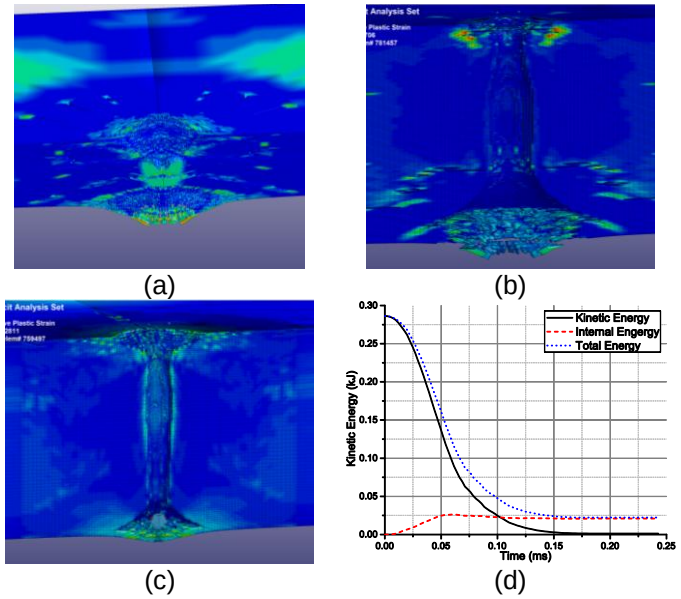

Figure 6: Cross-section of panels with *MAT_CSCM (a) 25-mm panel (b) 50-mm panel (c) 75-mm panel (d) Energy time-history in 75-mm panel

The spall/scab diameters and the depth of penetrations from numerical simulations were found to be consistent (Table 5) with the average experimental values. Specifically for the 75-mm panel, it was observed that the projectile was trapped and was partially visible through the scab. The same results were obtained from the numerical simulations and the projectile was visible within the panel after its kinetic energy was reduced to zero (Figure 6-(d)). It was established that the erosion criteria of 15% principal strain specified in *MAT_ADD_EROSION plays an important role. Erosion of elements is not a material property however it is essential in allowing the numerical solution to complete. Lower values of the percent principal strain resulted in complete perforation of the panel and higher values or not using erosion resulted in termination of the solution due to negative volume. The erosion parameter was also found to be mesh dependent and hence numerical results must be validated with experimental results before conducting parametric studies. Unlike other models, CSCM model provides an option for eroding elements only after damage, which is a material property. This option is recommended over *MAT_ADD_EROSION.

4.4.2 MAT72R3: Karagozian and Case Model

This model was not found appropriate for FMJ lead core projectile impact studies. The 25-mm panel and 50-mm panels were perforated with this model, however, the crater and scab dimensions were not accurate. In this constitutive model, the damage is implemented with three failure surfaces: yield, failure and residual and it is tracked by the damage accumulation factor. The damage accumulation starts after the yield surface is exceeded and the accumulation factor ranges from 0-1 when the material transitions between the yield surface and the maximum failure surface. Thereafter damage factor ranges from 1-2 as the material transitions between the maximum failure surface and residual failure surface (Malvar et al., 1997; Schwer & Malvar, 2005; User Manual L.S.T.C, 2015). The fringe plot for damage accumulation were not found to be consistent with the experimental results (Figure 7-(a)). Additionally, the solution for 75-mm and 100-mm panels terminated before completion with unusual results (Figure 7-(b)).

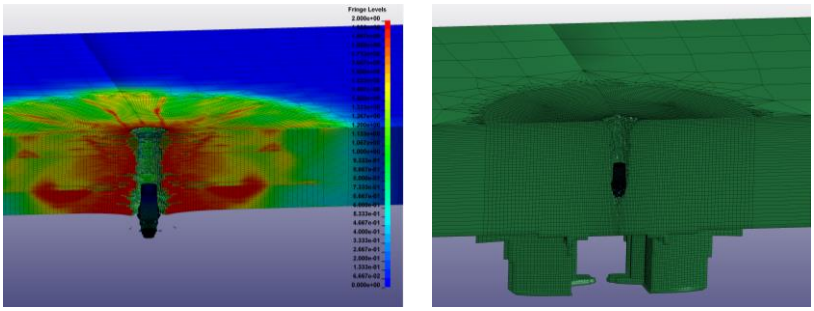

(a) (b)

Figure 7: Cross-section of panels with *MAT_72R3 (a) 25-mm panel (b) 75-mm panel

In another study by the authors on contact blast response of RC slab, the numerical solution completed without error when this model was used. However, the simulations showed complete perforation of the slab which was not consistent with the experimental results.

4.4.3 MAT084: Winfrith concrete model

This concrete model shows an elastic-perfectly plastic behavior in compressive loading and no strain softening is exhibited. Strain softening is included in tensile loading however it is found to be mesh sensitive. Winfrith model is not able to predict the shear dilation effect (Wu et al., 2012) hence not suitable for study of RC members where reinforcement bars confine the concrete. In this study, crater formation was not observed using this material model. However, 25-mm and 50-mm panels were perforated and scab formation was observed. The DOP of the projectile in 75-mm and 100-mm panels were less than the experimentally recorded values.

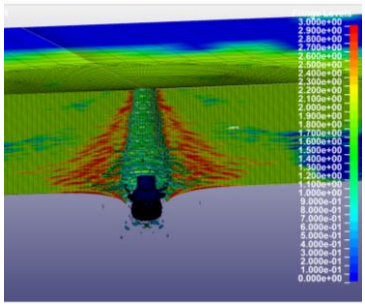

Figure 8: Cross section of 25-mm panel with *MAT_WINFRITH

5 Conclusions

Response of PC panels to projectile impact of 5.56 mm FMJ lead core bullets has been presented in this paper with an aim to identify an appropriate concrete constitutive model. Validation data collected from field tests has been compared to numerical results from LS-DYNA using three different concrete constitutive models. Constitutive models that can automatically generate material parameters from the unconfined concrete compressive strength were only considered.

Concrete exhibits strain-rate dependency on being subjected to high strain-rate loads. This is incorporated in the analytical design procedures by a dynamic increase factor (DIF) established from experimental observations (Telford, 1993). It was observed that this may not be necessary for numerical solutions. The increase in strength at high strain-rate is due to the confinement effect of concrete (Schwer, 2009). This aspect is inherently included in the numerical solutions. Hence it is not appropriate to include an additional increase in the strength for concrete constitutive model.

*MAT_CSCM (Mat_159) was found to simulate the impact studies with acceptable accuracy. With strain-rate effects deactivated, the damage fringe plot showed formation of crater and scab for all cases as observed in the experimental tests. It was found that erosion criteria is prudent in tackling the numerical instabilities arising due to large deformations. However, it has to be used with caution, as element erosion is not a material property and appropriate value has to be identified through validation with experimental results.

References

Andersen, C. E., Burkins, M. S., Walker, J. D., & Gooch, W. A. 2005. Time Resolved Penetration of B_4C Tiles by the APM2 Bullet. *Computer Modeling in Engineering & Sciences,* **8**(2): 91-104.

Børvik, T., Dey, S., & Clausen, A. H. 2009. Perforation Resistance of Five Different High-Strength Steel Plates Subjected to Small-Arms Projectiles. *International Journal of Impact Engineering,* **36**: 948-964.

Bush, B. M. 2010. *Analytical Evaluation of Concrete Penetration Modeling Techniques.* (Master of Science), North Carolina State University, North Carolina, USA.

Chen, W. F., & Han, D. J. 1988. *Plasticity for Structural Engineer*: Springer - Verlag. New York.

Cockcroft, M. G., & Latham, D. J. 1968. Ductility and the Workability of Metals. *Journal of the Institute of Metals,* **96**: 33-39.

Crawford, J. E., Magallanes, J. M., Lan, S., & Wu, Y. 2011. User's Manual and Documentation for Release III of the K&C Concrete Material Model in LS-DYNA. TR-11-36-1, Karagozian & Case.

Dey, S., Børvik, T., Hopperstad, O., Leinum, J., & Langseth, M. 2004. Effect of Target Strength on the Perforation of Steel Plates using Three Different Projectile Nose Shapes. *International Journal of Impact Engineering,* **30**(8-9): 1005-1038.

Dorsselaer, N. V., Lapoujade, V., Nahas, G., Tarallo, F., & Rambach, J.-M. 2012. *General Approach for Concrete Modelling: Impact on Reinforced Concrete*. 12th International LS-DYNA Users Conference: LSTC Detroit, USA.

Dua, A., & Braimah, A. 2016. *State-of-the-Art in Near-Field and Contact Explosion Effects on Reinforced Concrete Columns*. 5th International Structural Specialty Conference: Canadian Society for Civil Engineering London, Canada, pp. 1:12 (STR-836).

EN-1063. 1999. Glass in building, security glazing, testing and classification of resistance against bullet attack: European Standard.

Indian Army for Better Frontline Infrastructure. 2014, from http://defenceforumindia.com/forum/threads/indian-army-for-better-frontline-infrastructure.50840/page-5

Johnson, G. R., & Cook, W. H. 1983. *A Constitutive Model and Data for Metals Subjected to Large Strains, High Strain-Rates and High Temperatures*. Proceedings of Seventh Inernational Symposium on Ballistics: Hague, Netherlands.

LS-DYNA Support. 2016, Contact Modeling in LS-DYNA, from www.dynasupport.com.

Luccioni, B., Aráoz, G., & Labanda, N. 2013. Defining Erosion Limit for Concrete. *International Journal of protective structures,* **4**(3): 315-340.

Malvar, L., Crawford, J. E., Wesevich, J. W., & Simons, D. 1997. A Plasticity Concrete Material for DYNA3D. *International Journal of protective structures,* **19**(9-10): 847-873.

Manes, A., Bresciani, L. M., & Giglio, M. 2014. Ballistic Performance of Multi-Layered Fabric Composite Plates Impacted by Different 7.62 mm Calibre Projectiles. *Procedia Engineeing,* **88**: 208-215.

Maréchal, C., F, B., & G, H. 2011. Development of Numerical Model of the 9mm Parabellum FMJ Bullet Including Jacket Failure. *Engineering Transactions,* **59**(4): 263-272.

Murray, Y. D. 2007. User's Manual for LS-DYNA Concrete Material Model 159. FHWA-HRT-05-062, Federal Highway Administration.

Murthy, A. R. C., Palani, G. S., & Iyer, N. R. 2010. Impact Analysis of Concrete Structural Components (Review Paper). *Defence Science Journal,* **60**(3): 307-319.

Ottosen, N. S. 1975. *Failure and Elasticity of Concrete*: RISO - M1801.

Pavlovic, A., Fragassa, C., & Disic, A. 2016. Comparative Numerical and Experimental Study of Projectile Impact on Reinforced Concrete. *Composites Part B,* **108**: 122-130.

Peroni, L., Scapin, M., Fichera, C., Manes, A., & Giglio, M. 2012. Mechanical Properties at High Strain-Rate of Lead Core and Brass Jacket of a NATO 7.62 mm Ball Jacket. *EPJ Web of Conferences,* **26**: 1-6.

Prakash, A., Srinivasan, S. M., & Rao, A. R. M. 2015. Numerical investigation into steel fibre reinforced cementitious composite panels subjected to high velocity impact loading. *Materials and Design,* **83**: 164-175.

Schwer, L., & Malvar, L. 2005. *Simplified Concrete Modeling with *MAT_CONCRETE_DAMAGE_REL3*. JRI LS-DYNA User Week 2005: LSTC Nagoya, Japan.

Schwer, L. 2009. Strain-Rate Induced Strength Enhancement in Concrete: Much Ado About Nothing. *Proceedings of 7th European LS-DYNA Conference*: DYNAmore Salzburg, Austria

Telford, T. 1993. CEB-FIB Model Code 1990. Comité Euro-International du Béton, Lausanne, Switzerland.

User Manual L.S.T.C. 2015. LS-DYNA Keyword User's Manual, Volume II-Material Models. Livermore, California, USA: LSTC.

Williams, G. D., & Williamson, E. B. 2011. Response of Reinforced Concrete Bridge Columns Subjected to Blast Loads. *Journal of Structural Engineering,* **137**(9): 903-913.

Wilt, T., & Chowdhury, A. 2011. Response of Reinforced Concrete Structures to Aircraft Crash Impact. NRC-02-07-006, SouthWest Research Institute.

Wu, Y., Crawford, J. E., & Magallanes, J. M. 2012. *Performance of LS-DYNA Concrete Constitutive Models*. 12th International LS-DYNA Users Conference: LS-DYNA Dearborn, MI, USA.